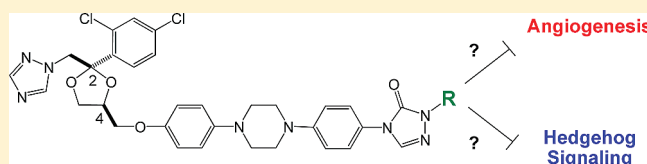


Itraconazole Side Chain Analogues: Structure–Activity Relationship Studies for Inhibition of Endothelial Cell Proliferation, Vascular Endothelial Growth Factor Receptor 2 (VEGFR2) Glycosylation, and Hedgehog Signaling

Wei Shi,[†] Benjamin A. Nacev,^{†,§,||} Blake T. Aftab,^{†,‡,||} Sarah Head,[†] Charles M. Rudin,[‡] and Jun O. Liu^{*,†,‡}[†]Department of Pharmacology and Molecular Sciences, [‡]Department of Oncology, [§]Medical Scientist Training Program, Johns Hopkins School of Medicine, 725 North Wolfe Street, Baltimore, Maryland 21205, United States

S Supporting Information

ABSTRACT: Itraconazole is an antifungal drug that was recently found to possess potent antiangiogenic activity and anti-hedgehog (Hh) pathway activity. To search for analogues of itraconazole with greater potency and to understand the structure–activity relationship in both antiangiogenic and Hh targeting activity, 25 itraconazole side chain analogues were synthesized and assayed for inhibition of endothelial cell proliferation and Gli1 transcription in a medulloblastoma (MB) culture. Through this analysis, we have identified analogues with increased potency for inhibiting endothelial cell proliferation and the Hh pathway, as well as VEGFR2 glycosylation that was recently found to be inhibited by itraconazole. An SAR analysis of these activities revealed that potent activity of the analogues against VEGFR2 glycosylation was generally driven by side chains of at least four carbons in composition with branching at the α or β position. SAR trends for targeting the Hh pathway were divergent from those related to HUVEC proliferation or VEGFR2 glycosylation. These results also suggest that modification of the *sec*-butyl side chain can lead to enhancement of the biological activity of itraconazole.



■ INTRODUCTION

Itraconazole is used as a clinical agent for the treatment of a broad spectrum of fungal infections. We previously found that itraconazole possesses potent antiangiogenic activity both in vitro and in vivo.^{1,2} In addition, it has been recently found that itraconazole inhibits Hh signaling and the growth of MB allografts with deregulated Hh activity.³ These reports form the basis for the expansion of the potential therapeutic application of itraconazole and have sparked evaluation of this agent in four ongoing cancer clinical trials.

To better understand the structural parameters that influence antiangiogenic activity, we have recently synthesized all eight stereoisomers of itraconazole (**1a–1h**, Figure 1).⁴ For the first time, these individual stereoisomers were evaluated for both their in vitro antiangiogenic and 14 α -demethylase inhibition (14DM)⁵ dependent antifungal activities.⁴ The discordance between these activities in one pair of *trans*-stereoisomers **1e–1f** and the others further supported our previous hypothesis that the molecular mechanism of itraconazole in antiangiogenesis is distinct from that for antifungal activity.¹

Our attempts to deconvolute the molecular basis of the antiangiogenic activity of itraconazole have revealed several cellular and biochemical effects in human umbilical vein endothelial cells (HUVEC). Itraconazole inhibits cholesterol trafficking in late endosomes/lysosomes and blocks mTORC1 and mTORC2 signaling.⁶ More recently, we observed that itraconazole can also impede the maturation of *N*-linked sugars appended to vascular endothelial

growth factor receptor 2 (VEGFR2) and blocks VEGF-activated phosphorylation of the receptor,² thereby blocking downstream signaling (Nacev et al., submitted for publication). Despite these new mechanistic insights, however, the direct target(s) of itraconazole remains unknown.

Itraconazole shares a large degree of structure similarity with the other azole antifungals, such as terconazole and ketoconazole (Figure 2), which, despite their equipotent antifungal activity in comparison to itraconazole, do not inhibit HUVEC proliferation¹ and fail to induce the VEGFR2 glycosylation defect (data not shown). The structural differences are particularly evident with respect to the triazolone ring and its *sec*-butyl side chain. This suggested that perhaps these moieties are responsible for the unique activities of itraconazole. Thus, we have synthesized a library of 25 itraconazole analogues in which the *sec*-butyl side chain was replaced by a group of substituents with diverse structural variations. These analogues were evaluated in several assays, including HUVEC proliferation, VEGFR2 glycosylation, medulloblastoma (MB) proliferation, and Hh signaling as measured by Gli1 transcript levels as a pharmacodynamic marker of pathway activation.

■ CHEMISTRY

The syntheses of itraconazole analogues **7a–7n** (Table 1) with linear, branched, or cyclic hydrocarbon side chains followed

Received: July 15, 2011

Published: September 21, 2011

the previously reported synthetic route (Scheme 1).⁴ Because the 2*S*,4*R*-*cis*-stereochemistry on the 1,3-dioxolane ring is most favored for antiangiogenic activity, one single diastereomer **6a**⁴ was used as the starting material to make the analogues unless otherwise stated.

Alkylated compounds **4a–4n** (Table 1) were prepared by reaction of the free triazolone precursor **2** with commercially available alkyl bromides or alkyl tosylates synthesized from commercially available alcohols (see the Supporting Information). For alkyl bromides or tosylates with a low boiling point, or potentially low stability or high reactivity at high temperatures, the reactions were carried out at room temperature with potassium carbonate and 18-crown-6. Demethylation of **4a–4n** with concentrated aqueous hydrobromic acid at 110 °C afforded the corresponding phenols **5a–5n** (Table 1) in excellent yields. Final coupling of **5a–5n** with 1,3-dioxolane tosylate **6a** gave the desired side chain analogues **7a–7n**.

The syntheses of analogues **7o–7q** (Table 2) are shown in Scheme 2. To incorporate the functional groups (azido, internal alkyne, and benzophenone) into the side chain, the methyl protecting group of the phenolic hydroxyl group was replaced with the methoxymethyl (MOM) group to avoid the harsh demethylation conditions (HBr, 110 °C). To start with, *N*-(4-hydroxyphenyl)-*N'*-(4-nitrophenyl)-piperazine **10** was prepared by heating the mixture of commercially available *N*-(4-hydroxyphenyl)-piperazine **8** and 1-chloro-4-nitrobenzene **9** in *N*-methylpyrrolidone (NMP) overnight.⁷ The crude product isolated from 2-propanol precipitation was directly used to react with methoxymethyl chloride to afford the MOM-protected intermediate **11**, which was purified by column chromatography. Subsequently, the nitro group in **11** was reduced to the amino group by refluxing with hydrazine monohydrate in the presence of 10% palladium on charcoal. In a three-step sequence, the aniline intermediate **12** was then reacted with phenyl chloroformate, hydrazine monohydrate, and formamide acetate to construct the triazolone ring in 51% yield over

three steps. Next, the *N*-alkylation of **13** with the corresponding alkylating reagents **3o–3q** (see the Supporting Information) under basic conditions afforded the intermediates **14a–14c** (Table 2), which were in turn treated with 50% trifluoroacetic acid in dichloromethane at room temperature to remove the MOM group. The acquired phenols **5o–5q** were subjected to the aforementioned coupling conditions to give the final products **7o–7q**.

Although the synthetic route described in Scheme 2 can accommodate a broad range of functional groups, two column purifications were usually required to remove DMSO and obtain the final products in good quality. To avoid the use of DMSO as the reaction solvent, we adopted a previously reported linear synthetic methodology (Scheme 3).⁸ The reaction sequence was first examined by using 2*R*,4*R*-*cis*-tosylate **6b** as the starting material due to its similar biological activity according to the reported stereoisomers.⁴ *N*-(4-hydroxyphenyl)-*N'*-(4-nitrophenyl)-piperazine **10** was purified by column chromatography before it was coupled with **6b**. Formation of the triazolone moiety in **17b** from the nitro group in **15b** was achieved by following the similar reaction conditions described in Scheme 2. Using potassium carbonate in combination with 18-crown-6 as the deprotonation reagents,⁹ the final *N*-alkylation of **17b** with 4-pentynyl-1-tosylate **3s** was performed in acetonitrile at 40 °C to give the final product **7r** in 63% yield. Similarly, analogues **7s–7x** (Table 3) were obtained from 2*S*,4*S*-*cis*-tosylate **6a** and the corresponding alkyl bromides or tosylates **3s–3x**.

RESULTS AND DISCUSSION

Inhibition of HUVEC Proliferation. We analyzed the previously determined activity of the analogues against HUVEC proliferation, which was used as an in vitro proxy for angiogenesis

Table 1. Side Chain Structures of Compounds **4a–4n**, **5a–5n**, and **7a–7n**

Compounds	R	Compounds	R
4a/5a/7a		4h/5h/7h^a	
4b/5b/7b		4i/5i/7i	
4c/5c/7c		4j/5j/7j	
4d/5d/7d		4k/5k/7k	
4e/5e/7e		4l/5l/7l	
4f/5f/7f		4m/5m/7m	
4g/5g/7g		4n/5n/7n	

^a Racemic on the side chain.

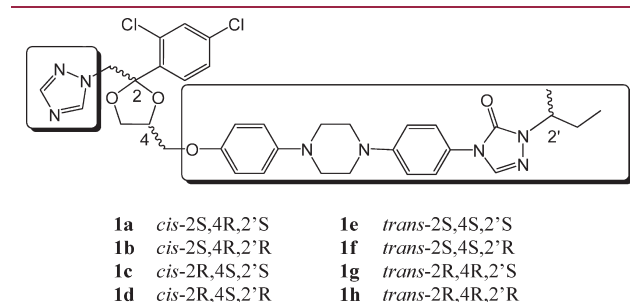
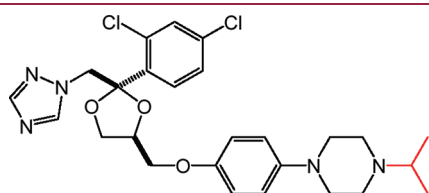
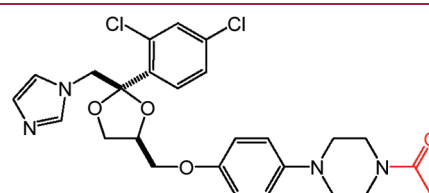


Figure 1. Structures of the eight itraconazole diastereomers arising from three stereogenic centers numbered 2, 4, and 2'. The *cis*- designation denotes that the two substituents in the boxes are on the same side of the 1,3-dioxolane ring, while *trans*- denotes the opposite orientation.³

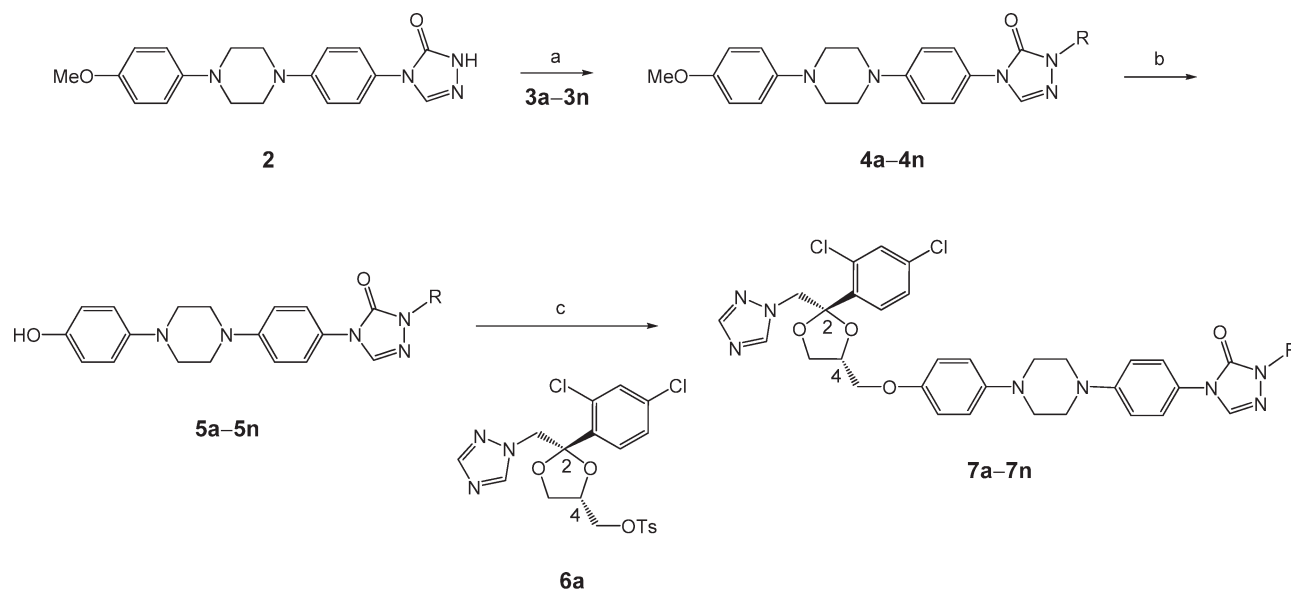


Terconazole



Ketoconazole

Figure 2. Structures of terconazole and ketoconazole.

Scheme 1^a

^a Reagents and conditions: (a) K_2CO_3 , 18-crown-8, DMSO, rt, or K_2CO_3 , KI, DMSO, 80 °C; (b) 48% aqueous HBr, 110 °C; (c) NaH, DMSO, 50 °C \rightarrow 85 °C.

inhibition (Table 3). From Table 3, it is clear that modification of the side chain in most analogues did not dramatically affect the activity. Those analogues with extremely short side chains (7a, and 7b) or lacking any side chain (17a) had lower potency for inhibition of HUVEC proliferation than itraconazole. A few analogues, however, possess considerably higher potency, including 7r and 7u.

The similar or even improved potency for compounds 7k, 7l, and 7v, all of which have bulky side chains, implies a putative binding site that is not sterically hindered. The relatively rigid conformation in 7o, 7s, and 7t further supports this idea and extends it to suggest that the binding pocket in the putative target may be quite deep. However, the loss of activity in 7w confounds this hypothesis. One possible explanation is that the loss of lipophilicity resulting from the incorporation of two nitrogens may have compromised activity. This is supported by the data for 7x in which an increase in lipophilicity appears to have compensated for the presence of the diazine. The near total loss of activity in 7q indicated that there is a limit to the size of the side chain with respect to inhibition of HUVEC proliferation.

Perhaps most notably, the potency of itraconazole against HUVEC proliferation was significantly increased by the incorporation of relatively small functional groups, such as the azido group in 7p, the terminal alkyne in 7r, and the cyano group in 7u. This implies that there are some interactions in the binding site of the side chain that are not utilized by the *sec*-butyl group in itraconazole. These results also suggested that substituents in place of the *sec*-butyl group of itraconazole can be further explored to optimize the potency of itraconazole.

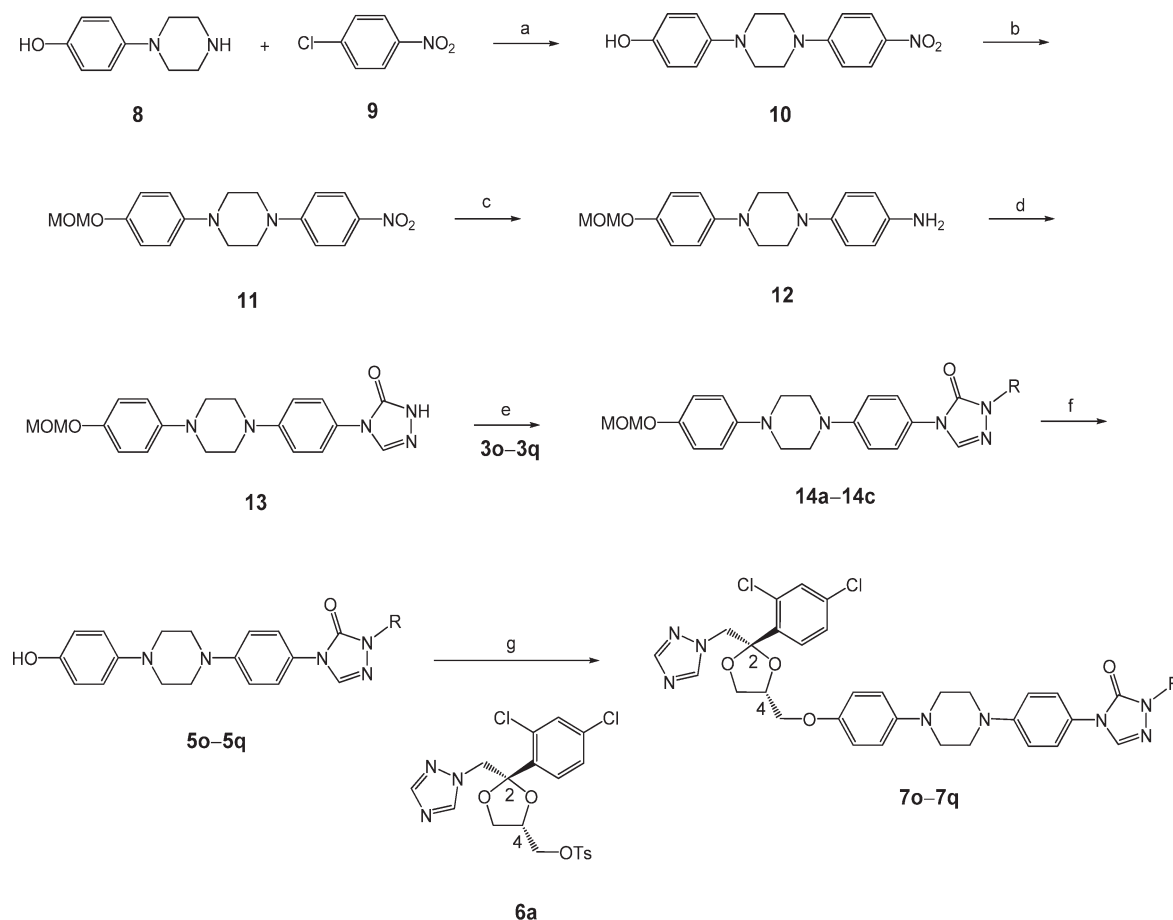
Inhibition of VEGFR2 Glycosylation. Having recently uncovered that itraconazole blocks the normal maturation of *N*-glycans on VEGFR2, we analyzed the influence of the side chain structure on this activity as well (Nacev et al., submitted for publication) (Table 3). VEGFR2 hypoglycosylation was scored either robust (++), intermediate (+), or absent (–) (Supporting Information Figure S1). Robust inhibitors of glycosylation had significantly

Table 2. Side Chain Structures of Compounds 14a–14c, 5o–5q, and 7o–7q

Compounds	Structure of the R group
14a/5o/7o	
14b/5p/7p	
14c/5q/7q	

($p < 0.05$) greater potencies against proliferation than the group in which the hypoglycosylation was absent, suggesting that this phenotype makes an overall contribution to inhibition of HUVEC proliferation (Table 4). We also observed that side chains comprised of four carbons or greater with branching at the α or β position strongly favored robust glycosylation inhibition compared to all other structural isomers (Figure 3). Compound 7j produced an intermediate glycosylation defect and was an exception to this rule. Compared to 7k, 7l, and 7v, the other analogues which contained bulky side chains and retained glycosylation inhibition, 7j had the greatest number of possible rotational isomers, suggesting that only certain conformations may be suitable for glycosylation inhibition.

Inhibition of Ptch^{-/+} Medulloblastoma Proliferation. Itraconazole has recently been reported to inhibit Hh pathway signaling in a 3T3 cell-based reporter system and in medulloblastoma allografts exhibiting Hh pathway-dependent growth.³ This reported activity against Hh signaling also seems to be unrelated to inhibition of 14DM, as other azole antifungal agents demonstrate decreased potency against this pathway, regardless of their activity on human 14DM. To explore the relation of the antiangiogenic and anti-Hh signaling capacity of itraconazole, we assessed the antiproliferative potency of the side chain analogues

Scheme 2^a

^a Reagents and conditions: (a) DIPEA, NMP, 125 °C; (b) MOMCl, DIPEA, rt, 79% over two steps; (c) 10% Pd/C, NH₂NH₂·H₂O, EtOH, reflux, 99%; (d) (i) phenyl chloroformate, pyridine, CH₃CN, (ii) NH₂NH₂·H₂O, 1,4-dioxane, reflux, (iii) formamidinium acetate, 1-propanol, 110 °C, 51% over 3 steps; (e) K₂CO₃, KI, DMSO, 80 °C; (f) TFA, 0 °C → rt; (g) NaH, DMSO, 50 °C → 85 °C.

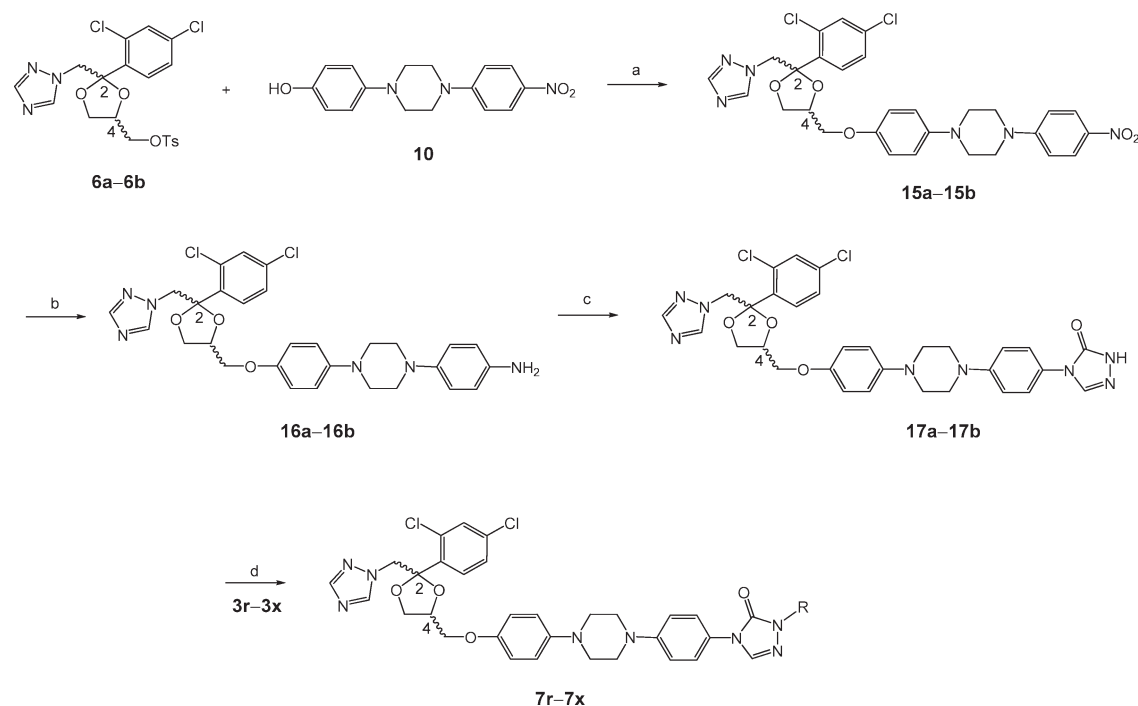
in MB cultures. These cultures were derived from Ptch^{-/+};p53^{-/-} mice that spontaneously develop medulloblastoma associated with ligand independent Hh pathway activation.¹⁰ IC₅₀ values for proliferation were determined for analogues and are represented as relative potencies compared to that of itraconazole (Table 3). Overall, there was poor correlation between analogue potency ratios for MB and HUVEC proliferation (Spearman $r = 0.327$; $p = 0.063$) (Figure 4). Notably, compounds **7q** and **7w**, which lost >69.9- and >13.8-fold of activity against HUVEC, respectively, had respective relative activities of 0.8 and 1.32 against MB proliferation when compared to itraconazole. Furthermore, the lack of data points in the lower right quadrant of Figure 4 illustrates that, without exception, all analogues demonstrating equivalent or increased potency against HUVEC proliferation with respect to itraconazole also demonstrate equivalent or increased potency against MB proliferation. These findings are consistent with the possibility that the target of itraconazole in HUVEC may also contribute to the potency of itraconazole against MB proliferation.

Inhibition of Hh Pathway Signaling. Inhibitors of the Hh pathway are known to inhibit MB cell proliferation. However, MB cell proliferation is also affected by drugs with targets other than Hh signaling. Therefore, to determine the extent to which the demonstrated potencies on MB proliferation are associated with Hh pathway inhibition, we exposed established MB colonies

to the itraconazole analogues at the IC₉₀ for MB proliferation and quantified transcript levels of Gli1, a transcriptional gene target of the Hh pathway. These data were then scored based on transcript levels associated with exposure of MB to synthetic inhibitors of the signaling protein Smoothened, HhAntag¹¹ and vismodegib (GDC-0449),¹² at the IC₉₀ for proliferation. The results are listed in Table 3.

Overall, there was a statistically significant association between inhibition of MB proliferation and inhibition of Hh pathway activity ($p = 0.05$; Supporting Information Figure S2). However, some analogues with relatively weak inhibition of Gli1 expression did demonstrate potent inhibition of MB proliferation, suggesting that in these instances, antiproliferative activity was predominantly Hh pathway independent.

There was no evident association between inhibition of VEGFR2 glycosylation and targeting of the Hh pathway (Supporting Information Figure S3). Nine of 10 analogues demonstrating strong inhibition of the Hh pathway did not inhibit VEGFR2 glycosylation. Furthermore, of the six strongest inhibitors of VEGFR2 glycosylation, two were not associated with Hh-dependent inhibition, three were intermediate inhibitors, and only one strongly inhibited Hh signaling. Notably, with the exception of compound **7h**, all analogues demonstrating strong inhibition of VEGFR2 glycosylation also demonstrated increased potency against MB

Scheme 3^a

^a Reagents and conditions: (a) NaH, DMF, 50 °C, 88%; (b) 10% Pd/C, $\text{NH}_2\text{NH}_2 \cdot \text{H}_2\text{O}$, EtOH, reflux, 99%; (c) (i) Phenyl chloroformate, pyridine, CH_3CN , (ii) $\text{NH}_2\text{NH}_2 \cdot \text{H}_2\text{O}$, 1,4-dioxane, reflux, (iii) formamidine acetate, 1-propanol, 110 °C, 48% over 3 steps; (d) K_2CO_3 , 18-crown-6, CH_3CN , 40 °C.

proliferation. These findings reveal a high level of discordance between these pharmacodynamic markers.

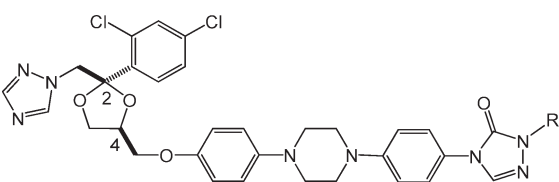
A study of side chain modifications associated with strong Hh pathway inhibition reveals several SAR trends. Analogues with side chains of three carbons or more in length without polar groups or branching at the β carbon demonstrated strong inhibition of Hh pathway activity (Figure 5). Compound 7e is an exception, as it was not associated with strong Hh pathway inhibition, which is somewhat surprising as structurally closely related analogues 7c and 7g exhibited strong Hh inhibition.

Examination of the side chains included in this defined set reveals that the criteria for potent inhibition of the Hh pathway is permissive to extension of the side chain beyond three carbons in length, as elongation up to *n*-octane (compound 7m) generally resulted in increased potency for Hh pathway inhibition and MB proliferation. Retention of potency for Hh pathway inhibition with compound 7n and loss of pathway specific activity with compound 7q suggests that there is some allowance for bulk at the distal end of these extensions but not to the extent necessary to accommodate a benzophenone group. This was similar to what we observed for HUVEC proliferation. Pathway inhibition was also permissive to branching on the α or γ carbon as demonstrated by Itra, 7h, 7i, and 7j. Compound 7k is an exception to this rule. This exception, in the context of the activity demonstrated by 7j, suggests that branching from the α position was not permissive to moieties with either large displacement volume or restricted rotational degrees of freedom. Pathway inhibition was also favored in compound 7r, containing a terminal alkyne. Alkene and alkyne linkages between γ and δ carbons were also active against the pathway.

Comparison of Structural Determinants for Inhibition of Hh Signaling, HUVEC Proliferation, and VEGFR2 Glycosylation. Taken together, the SAR trends and defined side chain sets derived from these analyses provide criteria for examining the relationship between activities against the Hh pathway and those targeting glycosylation and HUVEC proliferation. Overall, divergence between the activity of 7g and 7m demonstrate MB selectivity for saturated alkane chains greater than four carbons in length. Functional groups associated with the distal ends of 7n, 7p, and 7u further differentiate these activities and identify a preference for small, polar cyano, and azido functional groups in the pharmacophore associated with effects on HUVEC proliferation and VEGFR2 glycosylation, whereas a more bulky, hydrophobic phenyl group is preferred for activity against Hh signaling. Compounds 7k and 7l identify large groups proximal to the core triazolone ring as having improved activity in HUVEC proliferation and favoring inhibition of VEGFR2 glycosylation, whereas these structures were disfavored for inhibition of the Hh pathway. Interestingly, the *sec*-pentyl modification associated with compound 7h represents the only side chain composition in the analogue set that simultaneously inhibits glycosylation and the Hh pathway. Most notably, this compound was also the only analogue demonstrating increased potency across all parameters as compared with itraconazole.

CONCLUSION

Through *N*-alkylation of the triazolone moiety in three different synthetic routes, a focused library of 25 side chain analogues of itraconazole was synthesized. These analogues were screened for effects on HUVEC proliferation, VEGFR2 glycosylation, inhibition

Table 3. Inhibition of HUVEC Proliferation and VEGFR2 Glycosylation, MB Proliferation, and Gli1 Transcription by Itraconazole Stereoisomers 1a–1h and Side Chain Analogues 17a and 7a–7x^a


Compounds	R	Proliferation (IC ₅₀ /IC ₅₀ Itra)	Glycosylation (2 μM dose)	MB Proliferation (IC ₅₀ /IC ₅₀ Itra)	Gli1 Inhibition (IC ₅₀ Prolif. dose)
1a	2S,4R,2'S	0.8 ^{bf}	++	1.3 ^g	nd
1b	2S,4R,2'R	1.1 ^{bf}	++	1.4 ^g	nd
1c	2R,4S,2'S	1.6 ^{bf}	++	1.3 ^g	nd
1d	2R,4S,2'R	2.5 ^{bf}	++	1.7 ^g	nd
1e	2S,4S,2'S	3.1 ^{bf}	+	2.1 ^g	nd
1f	2S,4S,2'R	3.9 ^{bf}	–	1.7 ^g	nd
1g	2R,4R,2'S	3.2 ^{bf}	+	1.5 ^g	nd
1h	2R,4R,2'R	3.7 ^{bf}	–	2.3 ^g	nd
17a ^{c,d}	H	2.78 ^g	–	0.89 ^g	++
7a ^d		4.00 ^g	–	2.71 ^g	–
7b ^d		2.94 ^g	–	1.62 ^g	–
7c ^d		1.06	+	1.01	++
7d ^d		2.18 ^g	–	1.06	–
7e ^d		2.10	–	0.70 ^g	–
Itra ^f		1.00	++	1.00	++
7f ^d		1.32 ^g	++	0.86 ^g	–
7g		1.09	–	0.66 ^g	++
7h ^e		0.75	++	0.38 ^g	++
7i ^d		1.42 ^g	+	0.41 ^g	++
7j		1.10	+	0.54 ^g	++
7k		0.44 ^g	++	0.37 ^g	–
7l		0.50 ^g	++	0.50 ^g	+
7m		2.24 ^g	–	0.67 ^g	++
7n		1.45 ^g	–	0.69 ^g	++
7o		1.09	–	1.07	++
7p		0.30 ^g	+	0.70 ^g	+
7q		> 69.9	–	0.80 ^g	–
7r ^h		0.14 ^g	–	0.71 ^g	++
7s		1.57 ^g	–	0.63 ^g	++
7t		0.73	–	0.94	++
7u		0.18 ^g	++	0.84 ^g	+
7v		0.77	++	0.74 ^g	+
7w		> 13.8	+	1.32	+
7x		1.1 ^g	–	1.18	–

^a Stereochemistry on the 1,3-dioxolane ring is 2S,4R for 17a, 7a–7q, and 7s–7x and 2R,4S for 7r. ^b Proliferation data from ref 3. ^c Purity is 94.0%, t_R = 6.92 min; ^d Already reported in ref 7. ^e Mixture of the four *cis*-diastereomers, from Sigma-Aldrich. ^f Mixture of stereoisomers on the side chain. ^g EC₅₀/IC₅₀ Itra. This comparison was made for analogues with dose–response curves that did not reach zero proliferation even at the highest doses. ^h Indicates a lack of overlap between the 95% confidence interval for the un-normalized itraconazole reference IC₅₀ and the 95% CI for the analogue, which implies a statistically significant difference in the IC₅₀ values. ⁱ $p < 0.05$, F-test for differences in un-normalized log(IC₅₀ or EC₅₀) compared to the itraconazole reference value.

of Gli1 transcription in MB cells, and inhibition of MB proliferation. Analogues that were robust inhibitors of glycosylation were significantly associated with greater potency against HUVEC proliferation, suggesting that glycosylation inhibition contributes to the overall antiangiogenic activity of itraconazole. The SAR study on antiangiogenic activity suggests that the binding site of the side chain may be mainly hydrophobic and relatively deep and flexible. It was also possible to incorporate additional functional groups, such as terminal alkyne, azido, and cyano, which led to enhancement of antiangiogenic activity. However, to achieve potent inhibition against VEGFR2 glycosylation, there were more stringent structural and functional requirements for the side chain, mainly that side chains of at least four carbons with branching at the α or β position were generally required for high potency. Surprisingly, we found that some compounds with relatively potent inhibitory activity against MB proliferation were not similarly potent inhibitors of Gli1 transcription. Of the derivatives tested, 12 were found to exert strong Hh pathway inhibition associated with their antiproliferative effects in MB, as indicated by inhibition Gli1 transcript levels. These compounds were generally

Table 4. Correlation between HUVEC Proliferation Inhibition and Glycosylation Phenotype

glycosylation inhibition	–	+	++
<i>n</i>	10	7	16
mean IC ₅₀ ^a	6.3	3.4	1.0
mean Log ₂ (IC ₅₀ ^a)	1.0	0.9	–0.32
<i>p</i> -value ^{b,c}	N/A	0.83	0.04

^a Relative to Itraconazole (IC₅₀ analogue/IC₅₀ itraconazole). ^b *p*-Value calculated by a two-tailed Student's *t* test from log transformed data.

^c Compared to the “–” group.

defined as having side chains with extensions of at least three carbons in length and lacking branching from the β position. The distinct trends demonstrated by the SAR of these two molecular activities, together with the lack of correlation between the potency of the analogues in HUVEC and MB proliferation, suggest that itraconazole's effect on the Hh pathway is largely unrelated to the activity of itraconazole in HUVEC. It is possible that the effects of itraconazole on HUVEC and Hh signaling pathway are mediated

by distinct molecular targets. Together, the results presented herein have deepened our understanding of the role of the itraconazole side chain in the antiangiogenic and anti-Hh pathway activities of this drug and will likely facilitate the design of future analogues with increased potency for specific activities. Analogues with selectivity for one or more pathways may be useful in animal studies to clarify the role for each activity in *in vivo* tumor suppression.

EXPERIMENTAL SECTION

General. Reactions were carried out in oven-dried glassware. All reagents were purchased from commercial sources and were used without further purification unless noted. Unless stated otherwise, all reactions were carried out under a positive pressure of argon monitored by Merck precoated silica gel 60F-254 plates and visualized using 254 nm UV light. Column chromatography was performed on silica gel (200–400 mesh, Merck). The ratio between silica gel and crude product ranged from 100 to 50:1 (w/w). NMR data were collected on a Varian Unity-400 (400 MHz ^1H , 100 MHz ^{13}C) machine in the Department of Pharmacology and Molecular Sciences, the Johns Hopkins University. ^1H NMR spectra were obtained in deuteriochloroform (CDCl_3) with either tetramethylsilane (TMS, $\delta = 0.00$ for ^1H) or chloroform (CHCl_3 , $\delta = 7.27$ for ^1H) as an internal reference. ^{13}C NMR spectra were proton decoupled and were in CDCl_3 with either TMS ($\delta = 0.0$ for ^{13}C) or

CHCl_3 ($\delta = 77.0$ for ^{13}C) as an internal reference. Chemical shifts are reported in ppm (δ). Data are presented in the form: chemical shift (multiplicity, coupling constants, and integration). ^1H data are reported as though they were first-order. The errors between the coupling constants for two coupled protons were less than 0.5 Hz, and the average number was reported. Low-resolution mass spectra were obtained on a API 150EX single quadrupole LC/ESI-MS system in the Department of Pharmacology and Molecular Sciences or on a Voyager DE-STR, MALDI-TOF instrument at the AB Mass Spectrometry/Proteomics Facility at the Johns Hopkins University. The MALDI samples were prepared by mixing droplets of the sample solutions in chloroform or methanol and 2, 5-dihydroxybenzoic acid solution in acetone, where the latter served as the matrix. The reported purity values were obtained with a JASCO PU-2089S Plus quaternary pump system, using an MD-2010 Plus PDA detector at the wavelength of 256 nm and a Varian Microsorb-MV 100–5 C18 column. The eluant consisted of acetonitrile and 0.125% diethylamine in water, the ratio and flow rate of which depends on the compound. The purity of all final compounds synthesized is close to or above 95%. When the purity derived from HPLC analysis is greater than 99%, it is reported as >99%.

Typical Procedure A for the Preparation of 7a–7q. To a solution of the phenol 5a–5q (1 equiv) in DMSO was added NaH (a 60% dispersion in mineral oil, 4–5 equiv). After the mixture was stirred at 50 °C

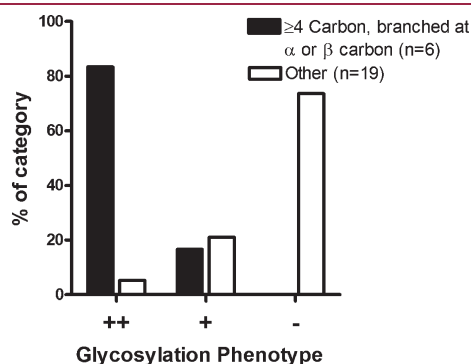


Figure 3. The number of carbons and branching of the itraconazole side chain influences the degree of glycosylation inhibition.

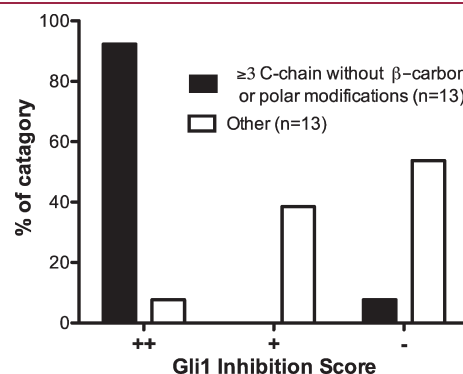


Figure 5. Length, branching, and polarity of the side chain influences Hh pathway inhibition.

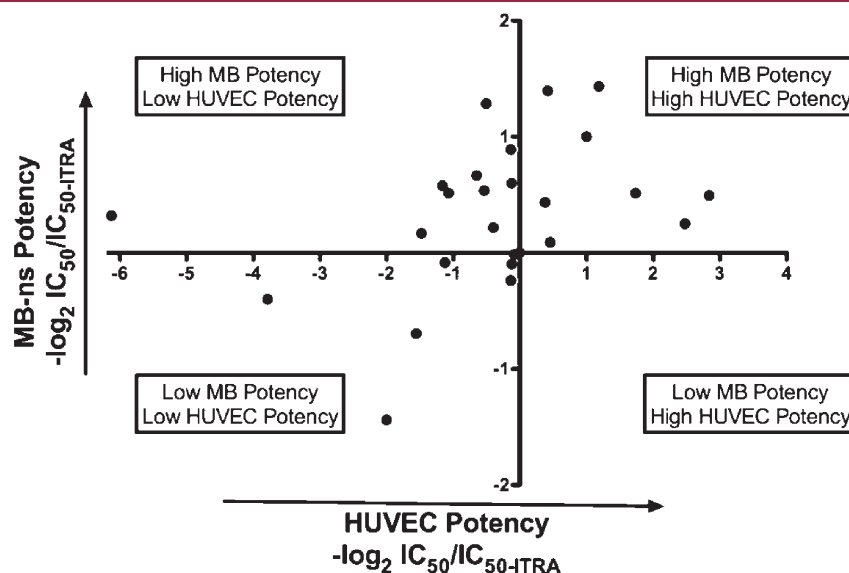


Figure 4. Lack of correlation between potency in MB and HUVEC proliferation.

under argon for 1 h, a solution of **6a** (1.05–1.1 equiv) in DMSO was added dropwise. After the addition, the temperature was increased to 90 °C and the solution was stirred under argon for another 3 h. The reaction was then quenched by the addition of a 50% aqueous NaCl solution, and the resulting mixture was extracted with CH₂Cl₂. The organic fractions were dried (Na₂SO₄), filtered, and concentrated under vacuum to yield the crude product, which was purified by column chromatography (1:1 hexanes–EtOAc → neat EtOAc) to afford the desired products, which could be further purified by a second column (neat CH₂Cl₂ → 50:1 CH₂Cl₂–CH₃OH) if necessary.

Typical Procedure B for the Preparation of 7r–7x. To a slurry of **17a** or **17b** (1 equiv) in acetonitrile was added **3r–3x** (1.3–1.6 equiv), K₂CO₃ (2 equiv), and 18-crown-6 (1 equiv). After the mixture was stirred at 40–50 °C under argon for 6–14 h, the solvent was removed under vacuum to yield the crude product, which was purified by column chromatography (neat CH₂Cl₂ → 50:1 CH₂Cl₂–CH₃OH).

cis-(2S,4R)-4-[4-[4-[4-[2-(2,4-Dichlorophenyl)-2-(1H-1,2,4-triazol-1-ylmethyl)-1,3-dioxolan-4-yl]methoxy]phenyl]l-piperazinyl]phenyl]-2,4-dihydro-2-methyl-3H-1,2,4-triazol-3-one (7a). This compound was synthesized as a colorless oil from **5a** (20.1 mg, 0.057 mmol), **6a** (29.1 mg, 0.060 mmol), and NaH (10.7 mg of a 60% dispersion in mineral oil, 0.27 mmol) in 41% yield by following typical procedure A. ¹H NMR (400 MHz, CDCl₃, δ_H) 8.20 (br s, 1H), 7.89 (br s, 1H), 7.63–7.55 (m, 2H), 7.49–7.36 (m, 3H), 7.25 (dd, *J* = 8.7, 2.4 Hz, 1H), 7.05–6.90 (m, 4H), 6.82–6.76 (m, 2H), 4.79 (q, *J* = 14.7 Hz, 2H), 4.40–4.32 (m, 1H), 3.94–3.88 (m, 1H), 3.85–3.75 (m, 2H), 3.52 (s, 3H), 3.46 (dd, *J* = 9.7, 6.4 Hz, 1H), 3.38–3.33 (m, 4H), 3.25–3.19 (m, 4H). ¹³C NMR (100 MHz, CDCl₃, δ_C) 152.82, 152.60, 151.61, 150.89, 146.20, 145.20, 136.28, 134.26, 133.34, 131.61, 129.84, 127.48, 125.92, 123.91, 118.69, 116.88, 115.47, 107.83, 74.91, 67.83, 67.65, 53.80, 50.80, 49.38, 32.90. MALDI-MS: 663.2 (*M* + *H*⁺), 685.2 (*M* + *Na*⁺). Purity: 98.5%, *t*_R = 6.56 min.

cis-(2S,4R)-4-[4-[4-[4-[2-(2,4-Dichlorophenyl)-2-(1H-1,2,4-triazol-1-ylmethyl)-1,3-dioxolan-4-yl]methoxy]phenyl]l-piperazinyl]phenyl]-2,4-dihydro-2-ethyl-3H-1,2,4-triazol-3-one (7b). This compound was synthesized as a colorless oil from **5b** (18.6 mg, 0.051 mmol), **6a** (27.7 mg, 0.057 mmol), and NaH (10.0 mg of a 60% dispersion in mineral oil, 0.25 mmol) in 58% yield by following typical procedure A. ¹H NMR (400 MHz, CDCl₃, δ_H) 8.21 (s, 1H), 7.90 (s, 1H), 7.67–7.53 (m, 2H), 7.49–7.37 (m, 3H), 7.25 (dd, *J* = 8.7, 2.3 Hz, 1H), 7.09–6.87 (m, 4H), 6.83–6.77 (m, 2H), 4.80 (q, *J* = 14.7 Hz, 2H), 4.46–4.27 (m, 1H), 3.99–3.73 (m, 5H), 3.46 (dt, *J* = 23.5, 11.8 Hz, 1H), 3.43–3.32 (m, 4H), 3.32–3.16 (m, 4H), 1.46–1.32 (t, *J* = 7.3 Hz, 3H). ¹³C NMR (100 MHz, CDCl₃, δ_C) 152.86, 152.11, 151.68, 150.84, 146.20, 136.29, 134.24, 133.35, 131.66, 129.84, 127.48, 126.02, 123.90, 118.71, 116.89, 115.49, 107.85, 74.92, 67.86, 67.67, 53.83, 50.82, 49.40, 40.79, 14.10. MALDI-MS: 677.2 (*M* + *H*⁺), 699.2 (*M* + *Na*⁺). Purity: >99%, *t*_R = 7.04 min.

cis-(2S,4R)-4-[4-[4-[4-[2-(2,4-Dichlorophenyl)-2-(1H-1,2,4-triazol-1-ylmethyl)-1,3-dioxolan-4-yl]methoxy]phenyl]l-piperazinyl]phenyl]-2,4-dihydro-2-propyl-3H-1,2,4-triazol-3-one (7c). This compound was synthesized as a colorless oil from **5c** (22.9 mg, 0.060 mmol), **6a** (32.0 mg, 0.066 mmol), and NaH (10.0 mg of a 60% dispersion in mineral oil, 0.25 mmol) in 53% yield by following typical procedure A. ¹H NMR (400 MHz, CDCl₃, δ_H) 8.24 (s, 1H), 7.90 (s, 1H), 7.65–7.54 (m, 2H), 7.47–7.38 (m, 3H), 7.25 (dd, *J* = 8.4, 2.1 Hz, 1H), 7.13–6.95 (m, 4H), 6.85–6.76 (m, 2H), 4.80 (q, *J* = 14.7 Hz, 2H), 4.45–4.28 (m, 1H), 3.97–3.73 (m, 5H), 3.60–3.10 (m, 9H), 1.94–1.68 (m, 2H), 0.97 (t, *J* = 7.4 Hz, 3H). ¹³C NMR (100 MHz, CDCl₃, δ_C) 152.38, 151.69, 150.59, 140.03, 136.29, 134.25, 134.12, 133.34, 131.66, 129.83, 127.49, 126.09, 123.80, 119.06, 117.02, 115.54, 107.85, 74.87, 67.81, 67.62, 53.81, 51.09, 49.23, 47.41, 22.26, 11.34. ESI-MS: 690.2 (*M* + *H*⁺), 712.2 (*M* + *Na*⁺). Purity: 97.4%, *t*_R = 7.45 min.

cis-(2S,4R)-4-[4-[4-[4-[2-(2,4-Dichlorophenyl)-2-(1H-1,2,4-triazol-1-ylmethyl)-1,3-dioxolan-4-yl]methoxy]phenyl]l-piperazinyl]phenyl]-2,4-dihydro-2-isopropyl-3H-1,2,4-triazol-3-one (7d). This compound was synthesized as a colorless oil from **5d** (26.9 mg, 0.066 mmol), **6a** (35.0 mg, 0.072 mmol), and NaH (10.9 mg of a 60% dispersion in mineral oil, 0.27 mmol) in 50% yield by following typical procedure A. ¹H NMR (400 MHz, CDCl₃, δ_H) 8.23 (s, 1H), 7.90 (s, 1H), 7.67–7.52 (m, 2H), 7.44–7.37 (m, 3H), 7.25 (dd, *J* = 8.3, 2.2 Hz, 1H), 7.07–6.89 (m, 4H), 6.84–6.75 (m, 2H), 4.81 (q, *J* = 14.6 Hz, 2H), 4.60–4.50 (m, 1H), 4.42–4.30 (m, 1H), 3.96–3.72 (m, 3H), 3.56–3.43 (m, 1H), 3.43–3.29 (m, 4H), 3.28–3.17 (m, 4H), 1.41 (d, *J* = 6.7 Hz, 6H). ¹³C NMR (100 MHz, CDCl₃, δ_C) 152.82, 152.09, 150.80, 146.23, 136.29, 134.27, 134.12, 133.37, 131.66, 129.84, 127.48, 126.06, 123.89, 118.69, 116.89, 115.49, 107.84, 74.92, 67.87, 67.68, 53.92, 50.82, 49.44, 47.17, 21.39. ESI-MS: 690.2 (*M* + *H*⁺), 712.2 (*M* + *Na*⁺). Purity: 94.7%, *t*_R = 8.63 min.

cis-(2S,4R)-4-[4-[4-[4-[2-(2,4-Dichlorophenyl)-2-(1H-1,2,4-triazol-1-ylmethyl)-1,3-dioxolan-4-yl]methoxy]phenyl]l-piperazinyl]phenyl]-2,4-dihydro-2-butyl-3H-1,2,4-triazol-3-one (7e). This compound was synthesized as a yellowish oil from **5e** (38.8 mg, 0.099 mmol), **6a** (52.6 mg, 0.11 mmol), and NaH (17.8 mg of a 60% dispersion in mineral oil, 0.45 mmol) in 52% yield by following typical procedure A. ¹H NMR (400 MHz, CDCl₃, δ_H) 8.21 (s, 1H), 7.89 (s, 1H), 7.64–7.52 (m, 2H), 7.46–7.38 (m, 3H), 7.24 (dd, *J* = 8.6, 2.2 Hz, 1H), 7.08–6.89 (m, 4H), 6.83–6.77 (m, 2H), 4.79 (q, *J* = 14.7 Hz, 2H), 4.42–4.28 (m, 1H), 3.98–3.71 (m, 5H), 3.48 (dd, *J* = 9.6, 6.3 Hz, 1H), 3.55–3.41 (m, 4H), 3.40–3.27 (m, 4H), 1.87–1.70 (m, 2H), 1.40 (dq, *J* = 14.7, 7.4 Hz, 2H), 0.96 (t, *J* = 7.4 Hz, 3H). ¹³C NMR (100 MHz, CDCl₃, δ_C) 152.83, 152.34, 151.55, 150.79, 146.22, 136.26, 134.28, 134.12, 133.34, 131.64, 129.83, 127.46, 126.07, 123.77, 118.67, 116.85, 115.51, 107.83, 74.93, 67.89, 67.66, 53.84, 50.79, 49.41, 45.55, 30.90, 20.00, 13.87. ESI-MS: 705.2 (*M* + *H*⁺), 727.2 (*M* + *Na*⁺). Purity: >99%, *t*_R = 9.89 min.

cis-(2S,4R)-4-[4-[4-[4-[2-(2,4-Dichlorophenyl)-2-(1H-1,2,4-triazol-1-ylmethyl)-1,3-dioxolan-4-yl]methoxy]phenyl]l-piperazinyl]phenyl]-2,4-dihydro-2-isobutyl-3H-1,2,4-triazol-3-one (7f). This compound was synthesized as a yellowish oil from **5f** (20.0 mg, 0.051 mmol), **6a** (27.1 mg, 0.058 mmol), and NaH (10.2 mg of a 60% dispersion in mineral oil, 0.26 mmol) in 63% yield by following typical procedure A. ¹H NMR (400 MHz, CDCl₃, δ_H) 8.22 (s, 1H), 7.89 (s, 1H), 7.66–7.51 (m, 2H), 7.48–7.37 (m, 3H), 7.25 (dd, *J* = 8.6, 2.2 Hz, 1H), 7.05–6.88 (m, 4H), 6.83–6.76 (m, 2H), 4.80 (q, *J* = 14.7 Hz, 2H), 4.41–4.29 (m, 1H), 3.91 (dd, *J* = 8.3, 6.7 Hz, 1H), 3.86–3.72 (m, 2H), 3.65 (d, *J* = 7.3 Hz, 2H), 3.47 (dd, *J* = 9.6, 6.4 Hz, 1H), 3.38–3.32 (m, 4H), 3.25–3.19 (m, 4H), 2.19 (dt, *J* = 13.7, 6.9 Hz, 1H), 0.97 (d, *J* = 6.7 Hz, 6H). ¹³C NMR (100 MHz, CDCl₃, δ_C) 152.82, 152.64, 150.79, 146.22, 136.28, 134.28, 134.06, 133.34, 131.65, 129.84, 127.47, 126.11, 123.72, 118.68, 116.88, 115.48, 107.83, 74.92, 67.86, 67.66, 53.87, 53.04, 50.80, 49.43, 28.46, 20.12. ESI-MS: 705.2 (*M* + *H*⁺), 727.2 (*M* + *Na*⁺). Purity: >99%, *t*_R = 9.63 min.

cis-(2S,4R)-4-[4-[4-[4-[2-(2,4-Dichlorophenyl)-2-(1H-1,2,4-triazol-1-ylmethyl)-1,3-dioxolan-4-yl]methoxy]phenyl]l-piperazinyl]phenyl]-2,4-dihydro-2-pentyl-3H-1,2,4-triazol-3-one (7g). This compound was synthesized as a yellowish oil from **5g** (23.4 mg, 0.057 mmol), **6a** (30.0 mg, 0.062 mmol), and NaH (11.4 mg of a 60% dispersion in mineral oil, 0.28 mmol) in 57% yield by following typical procedure A. ¹H NMR (400 MHz, CDCl₃, δ_H) 8.24 (s, 1H), 7.90 (s, 1H), 7.62–7.55 (m, 2H), 7.48–7.38 (m, 3H), 7.25 (dd, *J* = 8.3, 2.1 Hz, 1H), 7.15–6.95 (m, 4H), 6.85–6.77 (m, 2H), 4.80 (q, *J* = 14.7 Hz, 2H), 4.42–4.30 (m, 1H), 3.99–3.71 (m, 5H), 3.58–3.19 (m, 9H), 1.88–1.70 (m, 2H), 1.35 (dd, *J* = 7.2, 3.7 Hz, 4H), 0.90 (dd, *J* = 8.8, 5.0 Hz, 3H). ¹³C NMR (100 MHz, CDCl₃, δ_C) 152.32, 150.59, 136.31, 134.22, 134.12, 133.34, 131.67, 129.83, 127.50, 123.83, 117.07, 116.68, 115.57, 107.85, 74.86, 67.80, 67.60, 53.82, 51.42, 49.13, 45.85, 28.92,

28.58, 22.51, 14.21. ESI-MS: 719.3 ($M + H^+$), 741.3 ($M + Na^+$). Purity: >99%, $t_R = 13.19$ min.

cis-(2S,4R)-4-[4-[4-[4-[[2-(2,4-Dichlorophenyl)-2-(1H-1,2,4-triazol-1-yl)methyl]-1,3-dioxolan-4-yl]methoxy]phenyl]-lpiperazinyl]phenyl]-2,4-dihydro-2-(1-methylbutyl)-3H-1,2,4-triazol-3-one (7h). This compound was synthesized as a yellowish oil from **5h** (23.4 mg, 0.057 mmol), **6a** (29.8 mg, 0.062 mmol), and NaH (10.3 mg of a 60% dispersion in mineral oil, 0.26 mmol) in 66% yield by following typical procedure A. 1H NMR (400 MHz, $CDCl_3$, δ_H) 8.26 (s, 1H), 7.91 (s, 1H), 7.72–7.53 (m, 2H), 7.48–7.37 (m, 3H), 7.25 (dd, $J = 8.3, 2.1$ Hz, 1H), 7.13–6.96 (m, 4H), 6.86–6.79 (m, 2H), 4.81 (q, $J = 14.7$ Hz, 2H), 4.51–4.29 (m, 2H), 3.98–3.86 (m, 1H), 3.86–3.71 (m, 2H), 3.58–3.10 (m, 8H), 1.93–1.77 (m, 1H), 1.62 (ddt, $J = 13.6, 9.9, 5.9$ Hz, 1H), 1.47–1.18 (m, 6H), 0.92 (t, $J = 7.4$ Hz, 3H). ^{13}C NMR (100 MHz, $CDCl_3$, δ_C) 152.10, 150.56, 136.29, 134.23, 134.11, 133.34, 131.66, 129.83, 127.49, 123.75, 119.06, 117.05, 115.55, 107.84, 74.86, 67.80, 67.61, 53.84, 51.07, 49.24, 37.69, 29.93, 19.88, 19.70, 14.00. ESI-MS: 719.3 ($M + H^+$), 741.3 ($M + Na^+$). Purity: >99%, $t_R = 9.85$ min.

cis-(2S,4R)-4-[4-[4-[4-[[2-(2,4-Dichlorophenyl)-2-(1H-1,2,4-triazol-1-yl)methyl]-1,3-dioxolan-4-yl]methoxy]phenyl]-lpiperazinyl]phenyl]-2,4-dihydro-2-(3-methylbutyl)-3H-1,2,4-triazol-3-one (7i). This compound was synthesized as a yellowish oil from **5i** (23.4 mg, 0.057 mmol), **6a** (30.3 mg, 0.063 mmol), and NaH (11.1 mg of a 60% dispersion in mineral oil, 0.28 mmol) in 63% yield by following typical procedure A. 1H NMR (400 MHz, $CDCl_3$, δ_H) 8.23 (s, 1H), 7.90 (s, 1H), 7.67–7.51 (m, 2H), 7.51–7.34 (m, 3H), 7.25 (dd, $J = 8.4, 2.0$ Hz, 1H), 7.15–6.97 (m, 4H), 6.88–6.80 (m, 2H), 4.80 (q, $J = 14.7$ Hz, 2H), 4.43–4.27 (m, 1H), 3.98–3.70 (m, 5H), 3.56–3.08 (m, 9H), 1.73–1.60 (m, 3H), 0.96 (d, $J = 6.3$ Hz, 6H). ^{13}C NMR (100 MHz, $CDCl_3$, δ_C) 152.23, 150.60, 136.29, 134.24, 134.08, 133.34, 131.66, 129.83, 127.48, 123.76, 119.07, 117.03, 115.55, 107.84, 74.86, 67.81, 67.61, 53.83, 51.18, 49.21, 44.19, 37.56, 25.81, 22.61. ESI-MS: 719.3 ($M + H^+$), 741.3 ($M + Na^+$). Purity: >99%, $t_R = 10.10$ min.

cis-(2S,4R)-4-[4-[4-[4-[[2-(2,4-Dichlorophenyl)-2-(1H-1,2,4-triazol-1-yl)methyl]-1,3-dioxolan-4-yl]methoxy]phenyl]-lpiperazinyl]phenyl]-2,4-dihydro-2-(1-ethylpropyl)-3H-1,2,4-triazol-3-one (7j). This compound was synthesized as a yellowish oil from **5j** (23.3 mg, 0.057 mmol), **6a** (30.1 mg, 0.062 mmol), and NaH (10.4 mg of a 60% dispersion in mineral oil, 0.28 mmol) in 63% yield by following typical procedure A. 1H NMR (400 MHz, $CDCl_3$, δ_H) 8.26 (s, 1H), 7.91 (s, 1H), 7.69–7.53 (m, 2H), 7.51–7.37 (m, 3H), 7.25 (dd, $J = 8.4, 2.1$ Hz, 1H), 7.10–6.93 (m, 4H), 6.85–6.77 (m, 2H), 4.81 (q, $J = 14.7$ Hz, 2H), 4.47–4.29 (m, 1H), 4.12–3.99 (m, 1H), 3.99–3.86 (m, 1H), 3.87–3.71 (m, 2H), 3.57–3.13 (m, 9H), 1.94–1.62 (m, 4H), 0.88 (t, $J = 7.4$ Hz, 6H). ^{13}C NMR (100 MHz, $CDCl_3$, δ_C) 153.05, 150.53, 136.31, 134.22, 133.34, 131.67, 129.84, 127.50, 123.74, 119.15, 117.06, 115.57, 107.84, 74.87, 67.81, 67.61, 59.06, 53.86, 51.34, 49.22, 27.00, 10.97. ESI-MS: 719.3 ($M + H^+$), 741.3 ($M + Na^+$). Purity: 95.1%, $t_R = 9.17$ min.

cis-(2S,4R)-4-[4-[4-[4-[[2-(2,4-Dichlorophenyl)-2-(1H-1,2,4-triazol-1-yl)methyl]-1,3-dioxolan-4-yl]methoxy]phenyl]-lpiperazinyl]phenyl]-2,4-dihydro-2-(1-cyclohexyl)-3H-1,2,4-triazol-3-one (7k). This compound was synthesized as a yellowish oil from **5k** (21.8 mg, 0.052 mmol), **6a** (25.4 mg, 0.055 mmol), and NaH (10.0 mg of a 60% dispersion in mineral oil, 0.25 mmol) in 69% yield by following typical procedure A. 1H NMR (400 MHz, $CDCl_3$, δ_H) 8.20 (s, 1H), 7.88 (s, 1H), 7.71–7.51 (m, 2H), 7.47–7.36 (m, 3H), 7.24 (dd, $J = 8.7, 2.2$ Hz, 1H), 7.05–6.87 (m, 4H), 6.82–6.74 (m, 2H), 4.79 (q, $J = 14.7$ Hz, 2H), 4.40–4.28 (m, 1H), 4.20–4.05 (m, 1H), 3.98–3.71 (m, 3H), 3.46 (dd, $J = 9.6, 6.3$ Hz, 1H), 4.43–4.25 (m, 4H), 3.27–3.12 (m, 4H), 1.95–1.63 (m, 6H), 1.49–1.32 (m, 2H), 1.30–1.13 (m, 2H). ^{13}C NMR (100 MHz, $CDCl_3$, δ_C) 152.80, 151.73, 151.60, 150.75, 146.19, 136.26, 134.26, 134.04, 133.33, 131.64, 129.83, 127.48, 126.06, 123.89, 118.68, 116.87, 115.45, 107.82, 74.91, 67.82, 67.65, 54.31, 53.79,

50.80, 49.41, 31.69, 25.65, 25.45. ESI-MS: 731.3 ($M + H^+$), 753.3 ($M + Na^+$). Purity: >99%, $t_R = 7.77$ min.

cis-(2S,4R)-4-[4-[4-[4-[[2-(2,4-Dichlorophenyl)-2-(1H-1,2,4-triazol-1-yl)methyl]-1,3-dioxolan-4-yl]methoxy]phenyl]-lpiperazinyl]phenyl]-2,4-dihydro-2-(1-cyclopentylmethyl)-3H-1,2,4-triazol-3-one (7l). This compound was synthesized as a yellowish oil from **5l** (20.0 mg, 0.048 mmol), **6a** (25.4 mg, 0.052 mmol), and NaH (10.2 mg of a 60% dispersion in mineral oil, 0.26 mmol) in 68% yield by following typical procedure A. 1H NMR (400 MHz, $CDCl_3$, δ_H) 8.21 (s, 1H), 7.89 (s, 1H), 7.66–7.53 (m, 2H), 7.51–7.37 (m, 3H), 7.25 (dd, $J = 8.1, 1.7$ Hz, 1H), 7.14–6.89 (m, 4H), 6.82–6.72 (m, 2H), 4.80 (q, $J = 14.7$ Hz, 2H), 4.40–4.32 (m, 1H), 4.01–3.71 (m, 5H), 3.54–3.15 (m, 9H), 2.43 (dt, $J = 15.3, 7.6$ Hz, 1H), 1.95–1.47 (m, 6H), 1.40–1.25 (m, 2H). ^{13}C NMR (100 MHz, $CDCl_3$, δ_C) 152.83, 152.52, 151.61, 150.78, 146.21, 136.28, 134.27, 134.00, 133.34, 131.65, 129.84, 127.48, 126.12, 123.74, 118.70, 116.89, 115.48, 107.84, 74.92, 67.86, 67.66, 53.83, 50.81, 50.53, 49.44, 39.53, 30.36, 25.30. ESI-MS: 731.3 ($M + H^+$), 753.3 ($M + Na^+$). Purity: >99%, $t_R = 7.74$ min.

cis-(2S,4R)-4-[4-[4-[4-[[2-(2,4-Dichlorophenyl)-2-(1H-1,2,4-triazol-1-yl)methyl]-1,3-dioxolan-4-yl]methoxy]phenyl]-lpiperazinyl]phenyl]-2,4-dihydro-2-(n-octyl)-3H-1,2,4-triazol-3-one (7m). This compound was synthesized as a yellowish oil from **5m** (27.4 mg, 0.055 mmol), **6a** (29.3 mg, 0.060 mmol), and NaH (10.9 mg of a 60% dispersion in mineral oil, 0.27 mmol) in 72% yield by following typical procedure A. 1H NMR (400 MHz, $CDCl_3$, δ_H) 8.21 (s, 1H), 7.90 (s, 1H), 7.70–7.51 (m, 2H), 7.50–7.36 (m, 3H), 7.25 (dd, $J = 8.4, 1.9$ Hz, 1H), 7.13–6.90 (m, 4H), 6.84–6.73 (m, 2H), 4.80 (q, $J = 14.7$ Hz, 2H), 4.42–4.29 (m, 1H), 3.99–3.71 (m, 5H), 3.57–3.12 (m, 9H), 1.85–1.72 (dt, $J = 14.6, 7.4$ Hz, 2H), 1.48–1.16 (m, 10H), 0.87 (t, $J = 6.8$ Hz, 3H). ^{13}C NMR (100 MHz, $CDCl_3$, δ_C) 152.83, 152.33, 151.62, 150.81, 146.22, 136.29, 134.27, 134.11, 133.35, 131.66, 129.83, 127.47, 126.08, 123.80, 118.70, 116.89, 115.49, 107.85, 74.92, 67.86, 67.67, 53.84, 50.82, 49.43, 45.88, 32.00, 29.38, 28.88, 26.80, 22.86, 14.33. ESI-MS: 761.3 ($M + H^+$), 783.3 ($M + Na^+$). Purity: >99%, $t_R = 14.67$ min.

cis-(2S,4R)-4-[4-[4-[4-[[2-(2,4-Dichlorophenyl)-2-(1H-1,2,4-triazol-1-yl)methyl]-1,3-dioxolan-4-yl]methoxy]phenyl]-lpiperazinyl]phenyl]-2,4-dihydro-2-(6-phenylhexyl)-3H-1,2,4-triazol-3-one (7n). This compound was synthesized as a yellowish oil from **5n** (25.3 mg, 0.051 mmol), **6a** (25.9 mg, 0.054 mmol), and NaH (10.9 mg of a 60% dispersion in mineral oil, 0.27 mmol) in 70% yield by following typical procedure A. 1H NMR (400 MHz, $CDCl_3$, δ_H) 8.21 (s, 1H), 7.90 (s, 1H), 7.69–7.53 (m, 2H), 7.52–7.35 (m, 3H), 7.33–7.22 (m, 3H), 7.22–7.12 (m, 3H), 7.08–6.99 (m, 2H), 6.97–6.89 (m, 2H), 6.83–6.76 (m, 2H), 4.80 (q, $J = 14.7$ Hz, 2H), 4.39–4.32 (m, 1H), 4.01–3.72 (m, 5H), 3.47 (dd, $J = 9.7, 6.4$ Hz, 1H), 3.41–3.32 (m, 4H), 3.28–3.18 (m, 4H), 2.67–2.52 (d, $J = 7.5$ Hz, 2H), 1.83–1.72 (m, 2H), 1.70–1.56 (m, 2H), 1.46–1.33 (m, 4H). ^{13}C NMR (100 MHz, $CDCl_3$, δ_C) 152.82, 152.33, 151.62, 150.81, 146.20, 142.88, 136.28, 134.27, 134.17, 133.34, 131.66, 129.84, 128.62, 128.46, 127.49, 126.04, 125.83, 123.81, 118.70, 116.89, 115.47, 107.84, 74.92, 67.83, 67.66, 53.81, 50.81, 49.42, 45.81, 36.07, 31.53, 29.07, 28.83, 26.66. ESI-MS: 808.3 ($M + H^+$), 830.3 ($M + Na^+$). Purity: >99%, $t_R = 12.78$ min.

cis-(2S,4R)-4-[4-[4-[4-[[2-(2,4-Dichlorophenyl)-2-(1H-1,2,4-triazol-1-yl)methyl]-1,3-dioxolan-4-yl]methoxy]phenyl]-lpiperazinyl]phenyl]-2,4-dihydro-2-(hex-3-ynyl)-3H-1,2,4-triazol-3-one (7o). This compound was synthesized as a yellowish oil from **5o** (25.9 mg, 0.062 mmol), **6a** (31.6 mg, 0.065 mmol), and NaH (12.8 mg of a 60% dispersion in mineral oil, 0.32 mmol) in 65% yield by following typical procedure A. 1H NMR (400 MHz, $CDCl_3$, δ_H) 8.19 (s, 1H), 7.88 (s, 1H), 7.69–7.51 (m, 2H), 7.51–7.33 (m, 3H), 7.24 (dd, $J = 8.2, 2.0$ Hz, 1H), 7.06–6.87 (m, 4H), 6.79 (d, $J = 9.0$ Hz, 2H), 4.78 (q, $J = 14.7$ Hz, 2H), 4.48–4.25 (m, 1H), 4.06–3.72 (m, 5H), 3.54–3.12 (m, 9H), 2.63 (tt, $J = 7.3, 2.3$ Hz, 2H), 2.13 (qt, $J = 7.5, 2.3$ Hz, 2H), 1.17–0.99 (t, $J = 7.2$ Hz, 3H). ^{13}C NMR (100 MHz, $CDCl_3$, δ_C) 152.81,

152.25, 151.60, 150.84, 146.19, 145.15, 136.26, 134.51, 134.27, 133.33, 131.65, 129.84, 127.48, 125.92, 123.83, 118.68, 116.87, 115.46, 107.83, 83.95, 75.41, 74.91, 67.83, 67.65, 53.80, 50.79, 49.38, 45.02, 19.26, 14.34, 12.62. ESI-MS: 729.2 ($M + H^+$), 751.2 ($M + Na^+$). Purity: >99%, $t_R = 7.93$ min.

cis-(2S,4R)-4-[4-[4-[4-[2-(2,4-Dichlorophenyl)-2-(1H-1,2,4-triazol-1-yl)methyl]-1,3-dioxolan-4-yl]methoxy]phenyl]-lpiperazinyl]phenyl]-2,4-dihydro-2-(6-azidohexyl)-3H-1,2,4-triazol-3-one (7p). This compound was synthesized as a yellowish oil from **5p** (33.1 mg, 0.072 mmol), **6a** (36.4 mg, 0.075 mmol), and NaH (14.4 mg of a 60% dispersion in mineral oil, 0.36 mmol) in 44% yield by following typical procedure A. 1H NMR (400 MHz, $CDCl_3$, δ_H) 8.19 (s, 1H), 7.87 (s, 1H), 7.60 (s, 1H), 7.55 (d, $J = 8.4$ Hz, 1H), 7.44 (d, $J = 2.1$ Hz, 1H), 7.39 (t, $J = 6.0$ Hz, 2H), 7.23 (dd, $J = 8.4$, 2.1 Hz, 1H), 7.00 (d, $J = 9.0$ Hz, 2H), 6.93 (d, $J = 8.8$ Hz, 2H), 6.78 (d, $J = 9.0$ Hz, 2H), 4.77 (q, $J = 14.7$ Hz, 2H), 4.41–4.25 (m, 1H), 3.94–3.70 (m, 5H), 3.44 (dd, $J = 9.7$, 5.9 Hz, 1H), 3.41–3.30 (m, 4H), 3.28–3.16 (m, 6H), 1.88–1.71 (m, 2H), 1.65–1.52 (m, 2H), 1.45–1.33 (m, 4H). ^{13}C NMR (100 MHz, $CDCl_3$, δ_C) 152.93, 152.32, 151.59, 150.76, 136.24, 134.25, 133.32, 131.63, 129.84, 127.47, 126.00, 123.77, 118.75, 116.87, 115.47, 107.82, 74.90, 67.81, 67.62, 53.78, 51.53, 50.87, 49.33, 45.60, 28.91, 28.72, 26.50, 26.31. ESI-MS: 774.2 ($M + H^+$), 796.2 ($M + Na^+$). Purity: >99%, $t_R = 7.26$ min.

cis-(2S,4R)-4-[4-[4-[4-[2-(2,4-Dichlorophenyl)-2-(1H-1,2,4-triazol-1-yl)methyl]-1,3-dioxolan-4-yl]methoxy]phenyl]-lpiperazinyl]phenyl]-2,4-dihydro-2-(6-(4-benzoylphenoxy)hexyl)-3H-1,2,4-triazol-3-one (7q). This compound was synthesized as a yellowish oil from **5q** (38.8 mg, 0.063 mmol), **6a** (34.1 mg, 0.070 mmol), and NaH (12.3 mg of a 60% dispersion in mineral oil, 0.31 mmol) in 74% yield by following typical procedure A. 1H NMR (400 MHz, $CDCl_3$, δ_H) 8.22 (s, 1H), 7.89 (s, 1H), 7.84–7.77 (m, 2H), 7.73 (dd, $J = 8.3$, 1.2 Hz, 2H), 7.61 (s, 1H), 7.58–7.52 (m, 2H), 7.48–7.42 (m, 3H), 7.39 (d, $J = 8.9$ Hz, 2H), 7.24 (dd, $J = 8.4$, 2.0 Hz, 1H), 7.01 (d, $J = 9.0$ Hz, 2H), 6.93 (d, $J = 8.8$ Hz, 4H), 6.79 (d, $J = 8.8$ Hz, 2H), 4.79 (q, $J = 14.7$ Hz, 2H), 4.46–4.25 (m, 1H), 4.02 (t, $J = 6.4$ Hz, 2H), 3.96–3.71 (m, 5H), 3.47 (dd, $J = 9.5$, 6.4 Hz, 1H), 3.42–3.28 (m, 4H), 3.28–3.12 (m, 4H), 1.83 (dq, $J = 12.9$, 6.6 Hz, 4H), 1.64–1.36 (m, 4H). ^{13}C NMR (100 MHz, $CDCl_3$, δ_C) 195.78, 163.01, 152.82, 152.36, 151.68, 150.82, 146.21, 138.54, 136.26, 134.24, 133.33, 132.77, 132.05, 131.64, 130.11, 129.93, 129.84, 128.39, 127.47, 125.96, 123.77, 118.67, 116.84, 115.49, 114.23, 107.82, 74.92, 68.26, 67.86, 67.64, 53.86, 50.78, 49.37, 45.66, 29.14, 28.76, 26.46, 25.81. ESI-MS: 929.3 ($M + H^+$), 951.3 ($M + Na^+$). Purity: >99%, $t_R = 15.68$ min.

cis-(2R,4S)-4-[4-[4-[4-[2-(2,4-Dichlorophenyl)-2-(1H-1,2,4-triazol-1-yl)methyl]-1,3-dioxolan-4-yl]methoxy]phenyl]-lpiperazinyl]phenyl]-2,4-dihydro-2-(pent-4-ynyl)-3H-1,2,4-triazol-3-one (7r). This compound was synthesized as a yellowish oil from **17b** (25.6 mg, 0.039 mmol), **3r** (14.1 mg, 0.059 mmol), K_2CO_3 (10.9 mg, 0.079 mmol), and 18-crown-6 (10.4 mg, 0.039 mmol) in 40% yield by following typical procedure B. 1H NMR (400 MHz, $CDCl_3$, δ_H) 8.22 (s, 1H), 7.90 (s, 1H), 7.62 (s, 1H), 7.58 (d, $J = 8.4$ Hz, 1H), 7.48 (d, $J = 2.1$ Hz, 1H), 7.42 (dd, $J = 7.1$, 5.1 Hz, 2H), 7.25 (dd, $J = 8.7$, 2.3 Hz, 1H), 7.03 (d, $J = 9.1$ Hz, 2H), 6.94 (d, $J = 9.0$ Hz, 2H), 6.80 (d, $J = 9.0$ Hz, 2H), 4.81 (q, $J = 14.7$ Hz, 2H), 4.41–4.33 (m, 1H), 4.04–3.88 (m, 3H), 3.87–3.74 (m, 2H), 3.49 (dd, $J = 9.7$, 6.4 Hz, 1H), 3.42–3.34 (m, 4H), 3.27–3.19 (m, 4H), 2.32 (td, $J = 7.0$, 2.6 Hz, 2H), 2.11–1.96 (m, 3H). ^{13}C NMR (100 MHz, $CDCl_3$, δ_C) 152.84, 152.38, 151.68, 150.86, 146.24, 136.29, 134.35, 133.35, 131.66, 129.83, 127.47, 125.95, 123.79, 118.69, 116.86, 115.51, 107.85, 83.19, 74.93, 69.28, 67.89, 67.67, 53.87, 50.80, 49.40, 44.74, 27.71, 16.16. ESI-MS: 715.2 ($M + H^+$), 737.2 ($M + Na^+$). Purity: >99%, $t_R = 7.35$ min.

cis-(2S,4R)-4-[4-[4-[4-[2-(2,4-Dichlorophenyl)-2-(1H-1,2,4-triazol-1-yl)methyl]-1,3-dioxolan-4-yl]methoxy]phenyl]-lpiperazinyl]phenyl]-2,4-dihydro-2-((E)-hex-3-enyl)-3H-1,2,4-triazol-3-one (7s). This compound was synthesized as a yellowish oil

from **17a** (19.8 mg, 0.031 mmol), **3s** (12.3 mg, 0.048 mmol), K_2CO_3 (8.4 mg, 0.061 mmol), and 18-crown-6 (8.1 mg, 0.031 mmol) in 55% yield by following typical procedure B. 1H NMR (400 MHz, $CDCl_3$, δ_H) 8.23 (s, 1H), 7.90 (s, 1H), 7.61–7.55 (m, 2H), 7.51–7.37 (m, 3H), 7.25 (dd, $J = 8.4$, 1.8 Hz, 1H), 7.03 (d, $J = 9.0$ Hz, 2H), 6.95 (d, $J = 8.9$ Hz, 2H), 6.81 (d, $J = 8.9$ Hz, 2H), 5.50 (dtt, $J = 15.3$, 6.3, 1.3 Hz, 1H), 5.31–5.15 (m, 1H), 4.84 (q, $J = 14.7$ Hz, 2H), 4.49–4.32 (m, 1H), 3.92–3.73 (m, 6H), 3.52 (dd, $J = 9.7$, 6.5 Hz, 1H), 3.41–3.33 (m, 4H), 3.26–3.17 (m, 4H), 2.43 (q, $J = 7.0$ Hz, 2H), 2.08–1.92 (m, 2H), 0.92 (t, $J = 7.5$ Hz, 3H). ^{13}C NMR (100 MHz, $CDCl_3$, δ_C) 152.83, 152.36, 151.66, 150.85, 146.21, 136.28, 134.77, 134.29, 133.34, 131.67, 129.84, 127.49, 126.00, 124.52, 123.81, 118.70, 116.88, 115.48, 107.85, 74.92, 67.83, 67.66, 53.82, 50.82, 49.42, 45.57, 25.90, 21.82, 14.03. ESI-MS: 731.2 ($M + H^+$), 753.2 ($M + Na^+$). Purity: 95.3%, $t_R = 9.15$ min.

cis-(2S,4R)-4-[4-[4-[4-[2-(2,4-Dichlorophenyl)-2-(1H-1,2,4-triazol-1-yl)methyl]-1,3-dioxolan-4-yl]methoxy]phenyl]-lpiperazinyl]phenyl]-2,4-dihydro-2-((Z)-hex-3-enyl)-3H-1,2,4-triazol-3-one (7t). This compound was synthesized as a yellowish oil from **17a** (18.7 mg, 0.029 mmol), **3t** (11.0 mg, 0.043 mmol), K_2CO_3 (8.0 mg, 0.058 mmol), and 18-crown-6 (7.6 mg, 0.029 mmol) in 70% yield by following typical procedure B. 1H NMR (400 MHz, $CDCl_3$, δ_H) 8.21 (s, 1H), 7.89 (s, 1H), 7.62–7.55 (m, 2H), 7.50–7.36 (m, 3H), 7.25 (dd, $J = 8.5$, 1.7 Hz, 1H), 7.02 (d, $J = 9.0$ Hz, 2H), 6.94 (d, $J = 8.9$ Hz, 2H), 6.80 (d, $J = 8.9$ Hz, 2H), 5.50 (dt, $J = 10.7$, 7.2 Hz, 1H), 5.44–5.31 (m, 1H), 4.85 (q, $J = 14.7$ Hz, 2H), 4.48–4.30 (m, 1H), 3.95–3.75 (m, 6H), 3.49 (dd, $J = 9.9$, 6.3 Hz, 1H), 3.42–3.34 (m, 4H), 3.27–3.19 (m, 4H), 2.54 (q, $J = 7.0$ Hz, 2H), 2.12–1.97 (m, 2H), 0.93 (t, $J = 7.5$ Hz, 3H). ^{13}C NMR (100 MHz, $CDCl_3$, δ_C) 152.83, 152.34, 151.64, 150.84, 146.19, 136.29, 134.93, 134.21, 133.34, 131.66, 129.84, 127.49, 126.01, 124.33, 123.83, 118.71, 116.89, 115.47, 107.84, 74.92, 67.83, 67.66, 53.82, 50.82, 49.42, 45.60, 26.89, 20.80, 14.47. ESI-MS: 731.2 ($M + H^+$), 753.2 ($M + Na^+$). Purity: 95.0%, $t_R = 8.91$ min.

cis-(2S,4R)-4-[4-[4-[4-[2-(2,4-Dichlorophenyl)-2-(1H-1,2,4-triazol-1-yl)methyl]-1,3-dioxolan-4-yl]methoxy]phenyl]-lpiperazinyl]phenyl]-2,4-dihydro-2-(5-cyanopentyl)-3H-1,2,4-triazol-3-one (7u). This compound was synthesized as a yellowish oil from **17a** (40.0 mg, 0.062 mmol), **3u** (16.3 mg, 0.092 mmol), K_2CO_3 (17.1 mg, 0.124 mmol), and 18-crown-6 (16.3 mg, 0.062 mmol) in 41% yield by following typical procedure B. 1H NMR (400 MHz, $CDCl_3$, δ_H) 8.25 (s, 1H), 7.90 (s, 1H), 7.65–7.55 (m, 2H), 7.48 (d, $J = 1.7$ Hz, 1H), 7.41 (d, $J = 8.8$ Hz, 2H), 7.25 (dd, $J = 8.4$, 2.0 Hz, 1H), 7.03 (d, $J = 8.9$ Hz, 2H), 6.94 (d, $J = 8.7$ Hz, 2H), 6.81 (d, $J = 8.7$ Hz, 2H), 4.81 (q, $J = 14.7$ Hz, 2H), 4.50–4.25 (m, 1H), 4.05–3.71 (m, 5H), 3.49 (t, $J = 7.8$ Hz, 1H), 3.43–3.33 (m, 4H), 3.29–3.20 (m, 4H), 2.37 (t, $J = 7.1$ Hz, 2H), 1.93–1.81 (m, 2H), 1.80–1.69 (m, 2H), 1.60–1.49 (m, 2H). ^{13}C NMR (100 MHz, $CDCl_3$, δ_C) 152.85, 152.44, 150.91, 146.24, 136.30, 134.42, 134.28, 133.35, 131.66, 129.84, 127.48, 125.87, 123.87, 118.70, 116.87, 115.51, 107.83, 74.93, 67.89, 67.67, 53.95, 50.80, 49.39, 45.19, 28.01, 25.80, 25.15, 17.31. ESI-MS: 744.2 ($M + H^+$), 766.2 ($M + Na^+$). Purity: 94.9%, $t_R = 5.36$ min.

cis-(2S,4R)-4-[4-[4-[4-[2-(2,4-Dichlorophenyl)-2-(1H-1,2,4-triazol-1-yl)methyl]-1,3-dioxolan-4-yl]methoxy]phenyl]-lpiperazinyl]phenyl]-2,4-dihydro-2-((3-ethyloxetan-3-yl)methyl)-3H-1,2,4-triazol-3-one (7v). This compound was synthesized as a yellowish oil from **17a** (30.0 mg, 0.046 mmol), **3v** (18.7 mg, 0.069 mmol), K_2CO_3 (12.8 mg, 0.092 mmol), and 18-crown-6 (12.2 mg, 0.046 mmol) in 40% yield by following typical procedure B. 1H NMR (400 MHz, $CDCl_3$, δ_H) 8.21 (s, 1H), 7.90 (s, 1H), 7.72–7.52 (m, 2H), 7.52–7.36 (m, 3H), 7.25 (dd, $J = 8.5$, 2.2 Hz, 1H), 7.13–6.72 (m, 6H), 4.91–4.69 (m, 4H), 4.45 (d, $J = 6.3$ Hz, 2H), 4.41–4.32 (m, 1H), 4.07 (s, 2H), 3.92 (dd, $J = 8.3$, 6.7 Hz, 1H), 3.87–3.73 (m, 2H), 3.54–3.44 (m, 1H), 3.43–3.32 (m, 4H), 3.30–3.23 (m, 4H), 1.74 (dd, $J = 14.9$, 7.4 Hz, 2H), 1.00 (t, $J = 7.4$ Hz, 3H). ^{13}C NMR (100 MHz, $CDCl_3$, δ_C) 152.84, 151.60, 150.92, 146.20, 145.18, 136.28, 134.63, 134.27, 133.34, 131.65, 129.84, 127.48, 125.80, 123.79, 118.70, 116.87, 115.49,

107.84, 78.88, 74.92, 67.86, 67.66, 53.82, 50.80, 49.38, 49.26, 44.25, 27.57, 8.34. ESI-MS: 747.3 ($M + H^+$), 769.3 ($M + Na^+$). Purity: 94.6%, $t_R = 5.85$ min.

cis-(2S,4R)-4-[4-[4-[4-[2-(2,4-Dichlorophenyl)-2-(1H-1,2,4-triazol-1-ylmethyl)-1,3-dioxolan-4-yl]methoxy]phenyl]piperazinyl]phenyl]-2,4-dihydro-2-(2-(3-methyl-3H-diazirin-3-yl)ethyl)-3H-1,2,4-triazol-3-one (7w). This compound was synthesized as a yellowish oil from 17a (20.2 mg, 0.031 mmol), 3w (10.3 mg, 0.040 mmol), K_2CO_3 (8.6 mg, 0.062 mmol), and 18-crown-6 (8.2 mg, 0.031 mmol) in 55% yield by following typical procedure B. 1H NMR (400 MHz, $CDCl_3$, δ_H) 8.24 (s, 1H), 7.90 (s, 1H), 7.64 (s, 1H), 7.58 (d, $J = 8.4$ Hz, 1H), 7.48 (d, $J = 2.1$ Hz, 1H), 7.45–7.39 (m, 2H), 7.26 (dd, $J = 8.6, 2.1$ Hz, 1H), 7.04 (d, $J = 9.0$ Hz, 2H), 6.94 (d, $J = 8.6$ Hz, 2H), 6.81 (d, $J = 8.7$ Hz, 2H), 4.81 (q, $J = 14.7$ Hz, 2H), 4.43–4.31 (m, 1H), 3.98–3.85 (m, 3H), 3.85–3.75 (m, 2H), 3.49 (dd, $J = 9.4, 6.4$ Hz, 1H), 3.40–3.34 (m, 4H), 3.28–3.20 (m, 4H), 1.81 (t, $J = 7.1$ Hz, 2H), 1.10 (s, 3H). ^{13}C NMR (100 MHz, $CDCl_3$, δ_C) 152.84, 152.36, 150.95, 146.23, 136.29, 134.68, 134.28, 133.35, 131.66, 129.84, 127.47, 125.85, 123.95, 118.70, 116.87, 115.51, 107.84, 74.93, 67.88, 67.67, 53.90, 50.80, 49.39, 41.08, 33.91, 24.16, 19.57. ESI-MS: 731.2 ($M + H^+$), 753.2 ($M + Na^+$). Purity: 93.7%, $t_R = 9.84$ min.

cis-(2S,4R)-4-[4-[4-[4-[2-(2,4-Dichlorophenyl)-2-(1H-1,2,4-triazol-1-ylmethyl)-1,3-dioxolan-4-yl]methoxy]phenyl]piperazinyl]phenyl]-2,4-dihydro-2-(7-(3-methyl-3H-diazirin-3-yl)heptyl)-3H-1,2,4-triazol-3-one (7x). This compound was synthesized as a yellowish oil from 17a (21.9 mg, 0.034 mmol), 3x (16.4 mg, 0.051 mmol), K_2CO_3 (9.3 mg, 0.067 mmol), and 18-crown-6 (8.9 mg, 0.034 mmol) in 57% yield by following typical procedure B. 1H NMR (400 MHz, $CDCl_3$, δ_H) 8.22 (s, 1H), 7.90 (s, 1H), 7.64–7.52 (m, 2H), 7.52–7.33 (m, 3H), 7.25 (dd, $J = 8.5, 1.9$ Hz, 1H), 7.05–6.88 (m, 4H), 6.80 (d, $J = 8.6$ Hz, 2H), 4.80 (q, $J = 14.7$ Hz, 2H), 4.46–4.27 (m, 1H), 3.99–3.71 (m, 5H), 3.57–3.42 (m, 1H), 3.43–3.28 (m, 4H), 3.28–3.15 (m, 4H), 1.78 (dt, $J = 14.7, 7.3$ Hz, 2H), 1.44–1.08 (m, 10H), 1.02–0.92 (m, 3H). ^{13}C NMR (100 MHz, $CDCl_3$, δ_C) 152.84, 152.33, 150.81, 146.19, 136.28, 134.27, 134.16, 133.34, 131.65, 129.83, 127.47, 126.04, 123.80, 118.70, 116.88, 115.49, 107.84, 74.92, 67.86, 67.66, 53.86, 50.81, 49.41, 45.76, 34.47, 29.21, 29.15, 28.78, 26.59, 24.15, 20.11. ESI-MS: 801.3 ($M + H^+$), 823.3 ($M + Na^+$). Purity: 92.9%, $t_R = 10.84$ min.

HUVEC Culture and Proliferation Assays. Pooled HUVEC (Lonza) were grown in EGM-2 bullet kit media (Lonza) and used at passage eight or lower. The proliferation assays were conducted as previously described.¹³ GraphPad Prism (v4.00) was used to perform statistical comparisons of the IC_{50} and $\log(IC_{50})$ values for the itraconazole reference samples and the analogues.

VEGFR2 Glycosylation. HUVEC were seeded at 5×10^4 per well of a 6-well plate in 3 mL of media. After an overnight recovery, the media was replaced with 2 mL of fresh media and the analogues were added from 200X stocks in DMSO. Following a 24 h incubation, the media was aspirated and 2X SDS sample buffer was added to the cells, which were incubated on ice for 10 min and then boiled for 10 min. The lysate was then subjected to 6% SDS-PAGE and transferred to PVDF (Bio-Rad) membranes, which were subsequently blocked in 5% BSA (Sigma) in TBS-T (10 mM Tris pH 8.0, 150 mM NaCl, 0.05% Tween 20 [Sigma]) and then incubated with 1% anti-VEGFR2 in 1% BSA in TBS-T (Cell Signaling no. 2749). Following three washes in TBS-T, the membrane was incubated with antirabbit horseradish peroxidase conjugated IgG (GE Healthcare) (1:5000–1:10000 dilution) in 1% BSA in TBS-T. The membranes were washed three times in TBS-T, incubated for 1–5 min with ECL substrate (Immobilion Wester, Milipore), and visualized (Kodak Image Station 440 CF).

Medulloblastoma Culture. MB cultures were derived from mouse Ptc^{-/+}; p53^{-/-} MB grown as hind-flank allografts in nude mice (Harlan). Briefly, tumors were mechanically disrupted and made into single cell suspensions by two passages through a 70 μ m nylon filter. Cells were pelleted by centrifugation and resuspended in PBS pH 7.4 twice. The cell suspension was then subjected to centrifugation at 1000g for

25 min over a ficoll gradient. The viable cell layer formed at the ficoll boundary was then collected, suspended in PBS, and pelleted by centrifugation. The resulting pellet was then suspended and cultured as “neurospheres” in Neurobasal Media-A supplemented with retinoic acid deficient B-27 extract (NBMedia). Cells were cultured for three passages, with neurospheres disaggregated using Accumax (Innovative Cell Technologies) between passages. Prior to assaying, CD15 expression was confirmed by flow cytometric analysis. Inhibition of proliferation and Gli transcription was also confirmed in response to HhAntag and vismodegib (Supporting Information Figure S4).

Medulloblastoma Proliferation Assay. Cultured MB neurospheres were disaggregated as described and 1×10^4 cells were seeded into wells of a 96-well assay plate in NBMedia and exposed to multiple analogue concentrations. Relative cell numbers following a 96 h incubation were quantified by CellTiter 96 AQ_{ueous} One Solution Cell Proliferation Assay (Promega) per manufacturer's recommendations using a SpectraMax M2^e spectrophotometer and SoftMax Pro software (Molecular Devices). Data was analyzed using Prism5 (GraphPad Software) and IC_{50} and IC_{90} values were determined from dose–response curves fitted to mean corrected absorbance normalized to control treatment. GraphPad Prism (v5.0a) was used to perform statistical comparisons of the IC_{50} and $\log(IC_{50})$ values for the itraconazole reference samples and the analogues.

Quantification of Gli1 Transcript by TaqMan Analysis. MB neurospheres were cultured in NBMedia to confluence in 25 cm³ culture flasks and exposed for 24 h to analogues at the experimentally determined IC_{90} for proliferation. Following drug exposure, cells were washed in PBS and pelleted by centrifugation at 300g. Cell pellets were lysed in Trizol reagent (Invitrogen). Total RNA was separated and collected in the aqueous phase following centrifugation of lysate in the presence of chloroform. Total RNA was ethanol precipitated and purified over RNeasy Mini Kit (Qiagen) filter columns per manufacturer's recommendations. Transcript levels were quantified using gene-specific TaqMan primer/probe sets and the StepOne Plus Real-Time PCR system (Applied Biosystems) on cDNA reverse transcribed using the QuantiTect Reverse Transcription Kit (Qiagen) per manufacturers' recommendations. Results were quantified using StepOne Plus software v2.1 (Applied Biosystems) and were expressed as fold induction relative to control samples using the $\Delta\Delta Ct$ ($2^{-\Delta\Delta Ct}$) method with actin as an internal control. The primer/probe set (Applied Biosystems) for TaqMan PCR for mouse Gli-1 was Mm00494645_m1 and for mouse actin was Mm00607939_s1. Fold induction values for Gli1 transcript at the IC_{90} for MB proliferation were scored on a three-point semiquantitative scale as follows: ++, ≤ 0.15 ; +, 0.16–0.44; –, ≥ 0.45 .

■ ASSOCIATED CONTENT

S Supporting Information. Experimental procedures and analytical data for new compounds 3h, 3l, 3n–3t, 3v–3x, 4a–4n, 5a–5q, 11–13, and 14a–14c; VEGFR2 glycosylation scoring, characterization of MB culture system, experimentally determined IC_{90} , and associated $\Delta\Delta Ct$ values, and correlations between Gli1 inhibition and MB proliferation as well as VEGFR2 glycosylation. This material is available free of charge via the Internet at <http://pubs.acs.org>.

■ AUTHOR INFORMATION

Corresponding Author

*Phone: 410-955-4619. Fax: 410-955-4620. E-mail: joliu@jhu.edu.

Author Contributions

[†]These authors contributed equally to the work.

Notes

The authors report no conflicts of interest.

■ ACKNOWLEDGMENT

This work was supported by NCI, FAMRI, the Commonwealth Foundation, and a SPORE grant under NIH P50 CA058184 (J.O.L. and C.M.R.) and the NIH Medical Scientist Training Program grant T32GM07309 (B.A.N.). It was also supported in part by grant no. UL1 RR 025005 from the National Center for Research Resources (NCRR), a component of the National Institutes of Health (NIH) and NIH Roadmap for Medical Research, and its contents are solely the responsibility of the authors and do not necessarily represent the official view of NCRR or NIH.

■ ABBREVIATIONS USED

DIPEA, *N,N*-diisopropylethylamine; DMSO, dimethyl sulfoxide; EC₅₀, half maximal effective concentration; HBr, hydrobromic acid; Hh, hedgehog; HUVEC, human umbilical vein endothelial cells; IC₅₀, half maximal inhibitory concentration; IC₉₀, 90% maximal inhibitory concentration; Itra, itraconazole (commercial 1:1:1 mixture of *cis*-diastereomers); MB, medulloblastoma; MOMCl, methoxymethyl chloride; mTORC, mammalian target of rapamycin complex; NMP, methylpyrrolidone; SAR, structure–activity relationship; VEGFR2, vascular endothelial growth factor receptor 2; PCR, polymerase chain reaction

■ REFERENCES

- (1) Chong, C. R.; Lu, J.; Bhat, S.; Sullivan, D. J., Jr.; Liu, J. O. Inhibition of Angiogenesis by the Antifungal Drug Itraconazole. *ACS Chem. Biol.* **2007**, *2*, 263–270.
- (2) Aftab, B. T.; Dobromilskaya, I.; Liu, J. O.; Rudin, C. M. Itraconazole inhibits angiogenesis and tumor growth in non-small cell lung cancer. *Cancer Res.* **2011**, DOI: 10.1158/0008-5472.CAN-11-0691.
- (3) Kim, J.; Tang, J. Y.; Gong, R.; Lee, J. J.; Clemons, K. V.; Chong, C. R.; Chang, K. S.; Fereshteh, M.; Gardner, D.; Reya, T.; Liu, J. O.; Epstein, E. H.; Stevens, D. A.; Beachy, P. A. Itraconazole, a commonly used antifungal that inhibits hedgehog pathway activity and cancer growth. *Cancer Cell* **2010**, *17*, 388–399.
- (4) Shi, W.; Nacev, B. A.; Bhat, S.; Liu, J. O. Impact of Absolute Stereochemistry on the Antiangiogenic and Antifungal Activities of Itraconazole. *ACS Med. Chem. Lett.* **2010**, *1*, 155–159.
- (5) Vanden Bossche, H.; Marichal, P.; Gorrens, J.; Coene, M. C. Biochemical basis for the activity and selectivity of oral antifungal drugs. *Br. J. Clin. Pract. Suppl.* **1990**, *71*, 41–46.
- (6) Xu, J.; Dang, Y.; Ren, Y. R.; Liu, J. O. Cholesterol trafficking is required for mTOR activation in endothelial cells. *Proc. Natl. Acad. Sci. U.S.A.* **2010**, *107*, 4764–4769.
- (7) Giesinger, E. A. Process for preparing *N*-(4-hydroxyphenyl)-*N'*-(4'-aminophenyl)-piperazine. U.S. Patent US 6,355,801, 2002.
- (8) Heeres, J.; Backx, L. J.; Van Cutsem, J. Antimycotic azoles. 7. Synthesis and antifungal properties of a series of novel triazol-3-ones. *J. Med. Chem.* **1984**, *27*, 894–900.
- (9) Tanoury, G. J.; Hett, R.; Wilkinson, H. S.; Wald, S. A.; Senanayake, C. H. Total synthesis of (2*R*,4*S*,2'*S*,3'*R*)-hydroxyitraconazole: implementations of a recycle protocol and a mild and safe phase-transfer reagent for preparation of the key chiral units. *Tetrahedron: Asymmetry* **2003**, *14*, 3487–3493.
- (10) (a) Wetmore, C.; Eberhart, D. E.; Curran, T. Loss of p53 but not ARF accelerates medulloblastoma in mice heterozygous for patched. *Cancer Res.* **2001**, *61*, 513–516. (b) Berman, D. M.; Karhadkar, S. S.; Hallahan, A. R.; Pritchard, J. I.; Eberhart, C. G.; Watkins, D. N.; Chen, J. K.; Cooper, M. K.; Taipale, J.; Olson, J. M.; Beachy, P. A. Medulloblastoma growth inhibition by hedgehog pathway blockade. *Science* **2002**, *297*, 1559–1561. (c) Ward, R. J.; Lee, L.; Graham, K.; Satkunendran, T.; Yoshikawa, K.; Ling, E.; Harper, L.; Austin, R.; Nieuwenhuis, E.; Clarke, I. D.; Hui, C. C.; Dirks, P. B. Multipotent CD15+ cancer stem cells in patched-1-deficient mouse medulloblastoma. *Cancer Res.* **2009**, *69*, 4682–4690.
- (11) Romer, J. T.; Kimura, H.; Magdaleno, S.; Sasai, K.; Fuller, C.; Baines, H.; Connelly, M.; Stewart, C. F.; Gould, S.; Rubin, L. L.; Curran, T. Suppression of the Shh pathway using a small molecule inhibitor eliminates medulloblastoma in Ptc1(±)p53(–/–) mice. *Cancer Cell* **2004**, *6* (3), 229–240.
- (12) Von Hoff, D. D.; LoRusso, P. M.; Rudin, C. M.; Reddy, J. C.; Yauch, R. L.; Tibes, R.; Weiss, G. J.; Borad, M. J.; Hann, C. L.; Brahmer, J. R.; Mackey, H. M.; Lum, B. L.; Darbonne, W. C.; Marsters, J. C.; de Sauvage, F. J.; Low, J. A. Inhibition of the Hedgehog Pathway in Advanced Basal-Cell Carcinoma. *New Engl. J. Med.* **2009**, *361*, 1164–1172.
- (13) Nacev, B.; Low, W. K.; Huang, Z.; Su, T.; Su, Z.; Alkuraya, H.; Kasuga, D.; Sun, W.; Trager, M.; Braun, M.; Fischer, G.; Zhang, K.; Liu, J. O. A calcineurin-independent mechanism of angiogenesis inhibition by a non-immunosuppressive Cyclosporin A analog. *J. Pharmacol. Exp. Ther.* **2011**, *338*, 466–475.